J Fluoresc (2015) 25:1813–1818
DOI 10.1007/s10895-015-1671-5

ORIGINAL ARTICLE

Analysis of the Fluorescence Correlation Function of Quantum Rods with Different Lengths

Jaeran Lee[1] · **Sok Won Kim**[1]

Received: 24 July 2015 / Accepted: 14 September 2015 / Published online: 23 September 2015

Abstract We built a polarization fluorescence correlation spectroscopy system to analyze the variation of the correlation function in rotational diffusion based on the length of rod-like fluorescent particles. Because the rotational diffusion of particles in liquid depends on the relative polarization states of the laser source and particle fluorescence, we compared the amplitudes of the rotational diffusion using the autocorrelation function in different polarization states. For experiments that depend on the length of the fluorescent particles, we prepared three kinds of quantum rod samples with a width of 6.5±0.5 nm and lengths of 17±3, 40±3, and 46±3 nm. Through the experiment, we obtained the hydrodynamic radii of each particle using the rotational diffusion coefficient: 10.7±0.8, 13.4±0.7, and 14.1±0.4 nm with the length of the particles. All the obtained values for radii are 3 nm larger than the calculated equivalent radii of spheres with the same volume as the rod samples. Through a fraction analysis by polarization state, we confirmed that the ratio of rotational fraction for polarization increases with the aspect ratio of the actual particle.

Keywords Rod-like particle · Fluorescence · Correlation function · Polarization

Introduction

Fluorescence correlation spectroscopy (FCS) is a useful technique for quantitatively confirming the dynamic behavior of various molecules and analyzing the biological and chemical reaction mechanisms of molecules using fluorescent particles [1, 2]. Even though it is not a technique that observes variation in the micro-region, such as confocal microscopy, it can compare normalized dynamic sizes or speeds because the motion of particles much smaller than micrometer size can appear based on the quantitative diffusion coefficient [3]. Such quantitative information about particles is obtained by analyzing part of the translational diffusion using a correlation function of signals from the fluorescent particles [4]; however, if the rotational diffusion is also analyzed, more information about the motion of particles can be obtained [5, 6]. The translational diffusion region in the correlation function provides translational diffusion time, concentration of particles in solution, and viscosity with the size of the observation region, and the rotational diffusion region provides rotational diffusion time and characteristics of particle shape [7].

Studies using FCS generally investigate the diffusion motion of the test material attached with fluorescent probes or auto-fluorescent particles in solution. In many cases, though the shapes of the fluorescent probes are spheres, such as fluorescent beads and quantum dots [8, 9], rod-like particles such as quantum rods are also used as comparison targets to confirm the rotational diffusion property of the particles. Quantum rods are being actively studied because they can maintain a high quantum yield as quantum dots and can be made with various lengths. The analysis of the correlation function from fluorescent quantum rods can be used as a reference in analyzing the diffusion of rod-like particles; however, the blinking effect of quantum dots on the correlation function of quantum rods is not yet known [10].

In this study, we measured the rotational diffusion coefficients of fluorescent particles with three different lengths made in a core/shell structure of CdS/CdSe and compared the hydrodynamic radii of three kinds of particles. We also

✉ Sok Won Kim
sokkim@ulsan.ac.kr

[1] Department of Physics, University of Ulsan, Ulsan 680-749, South Korea

discuss the rotational fraction of the function for the two vertical polarization states.

Theory

The beam illuminated from a light source formed a focal volume with a few femto liters in solutions including fluorescent particles. When the particles come into the volume, they are excited and emit fluorescence. The fluorescence intensity emitted from them depends on the number, speed, and size of those particles diffusing into and out of the volume. This diffusion of the particles in the focal volume causes time-dependent fluctuations in fluorescence intensity. The fluctuations reflect information for their size, shape, number, and diffusing speed in the solution. The fluctuations caused by random diffusion of the fluorescent particles can be analyzed by a correlation function.

The fluorescence correlation function is the fluorescence intensity variation ($\delta F_1(t)$, $\delta F_2(t)$) from fluorescent particles converted into the form of an autocorrelation function or cross-correlation function. It can be represented as Eq. (1)

$$G(\tau) = \frac{\langle \delta F_1(t) \delta F_2(t+\tau) \rangle}{\langle F_1(t) \rangle \langle F_2(t) \rangle}, \tag{1}$$

where τ is delay time and $\langle\ \rangle$ is the time average of the time series signals. In Eq. (1), the correlation function was composed by increasing or decreasing regions regarding the emissive and dynamic properties of fluorescent particles. The well-known correlation function includes anti-bunching, triplet state, rotational and translational diffusion regions [11–13] and the model considered here includes only the diffusion effect of particles is represented by Eq. (2)

$$G(\tau) = \left[1 + R\ \mathrm{e}^{-\tau/\tau_R}\right] \cdot \left[G(0) \left(1 + \left(\frac{\tau}{\tau_D}\right)^{\alpha}\right)^{-1} \left(1 + \left(\left(\frac{w}{z}\right)^2 \left(\frac{\tau}{\tau_D}\right)\right)^{\alpha}\right)^{-1/2} \right], \tag{2}$$

where the terms inside [] are of rotational and translational diffusion, respectively [14]. The translational and rotational diffusion regions are the time regions caused by the particle diffusing into and out of the volume and, rotation, respectively. The τ_R and τ_D are the characteristic times of each region, R is rotational fraction, $G(0)$ is initial amplitude of the translational region, w/z is a value related to the structure of the focal volume, and α is an anomalous diffusion exponent. α determines the characteristics of diffusion such as super-diffusion, normal diffusion and sub-diffusion in the general complex system that does not conform to Fick's law [15]. In the translational diffusion term, $G(0)$ includes information about the concentration of particles. In the rotational diffusion term, it is well known that R depends on the polarization states of the light source and fluorescence; however, the relationship between R and the actual particle size is not clearly understood [14].

Experiments

We converted the FCS system into a polarization FCS-setup by adding a polarization system as shown Fig. 1. The position and role of the polarizers has been confirmed previously [7, 16]. To compose the polarization FCS-setup, we used a diode-pumped solid-state (DPSS) laser (Cobolt Samba; 25 mW) with a wavelength of 532 nm, a linear polarizer, polarizing beam splitter, and single-photon counting module (Id Quantique, id100-50), and time-correlated single-photon counter (PicoQuant, Time-harp 260).

In this polarized FCS-setup, the laser beam passes a linear polarizer, ND filter (neutral density filter), and two lens (to expand beam diameter) and enter the optical microscope (Olympus IX71). In microscope, the beam passes the excitation filter (Semrock, FF01-531/40-25) and reflects off the dichroic mirror (Semrock, FF545/605-Di02), and pass the objective lens (Olympus, 60×, 1.2 NA, water), the immersion water, and cover glass, and then focuses inside the sample solution. Before reached the objective lens, the laser intensity reduced by ND filter is 10 μW. Fluorescent particles inside the beam path are emitting fluorescent light in several different directions. A portion of this light enters the objective lens, after the light passes the dichroic mirror, emission filter (Semrock, FF01-593/40-25), and lens, it escapes the microscope by the inner mirror. A pinhole with diameter of 50 μm was placed in focal point of the microscope inner lens, and was passed only the fluorescent light emitted in focal point of objective lens. The light goes without spreading by a lens, and next lens was collected light in core of optical fiber. A polarizing beam splitter (PBS) between a lens and optical fiber separate the fluorescent light into two vertical polarized lights; The XXX denotes linearly polarized excitation and fluorescent light, and XYY indicates that the polarization states of the linearly polarized excitation light and the fluorescent light crossed [7]. In this system, two optical fibers and two single photon counting module (SPCM)s were used to obtain the

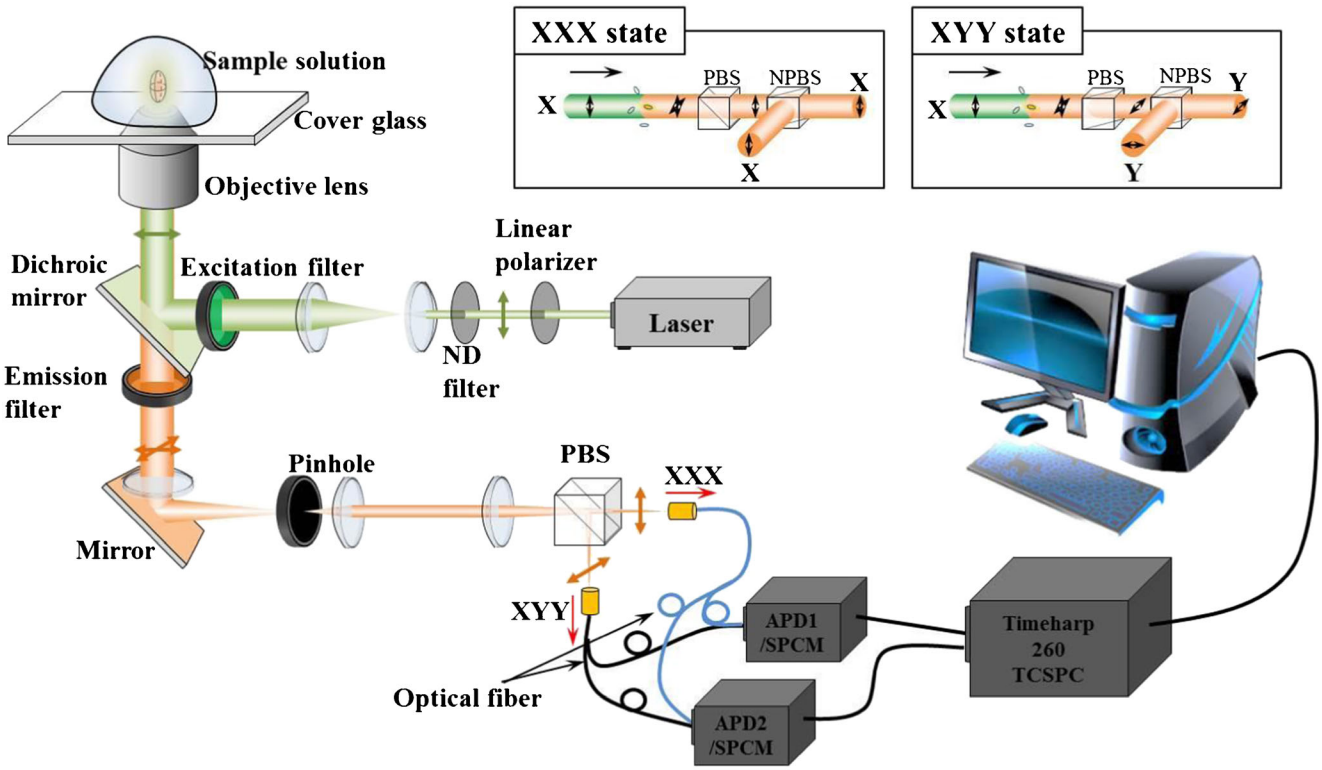

Fig. 1 Optical setup of polarized fluorescence correlation spectroscopy

cross-correlation data from two different detectors. In Here, the core diameter of optical fiber is 62.5 μm and splitting ratio of the fiber is 50:50. By the polarization state selection, the optical fibers are coupled or uncoupled with the SPCM. The fluorescent photons reached at SPCMs are converted into TTL(transistor-transistor logic) signals, which are then converted into a correlation function by using a time-correlated signal-photon counting (TCSPC) system. The correlation function is monitored by the Timharp260 program (PicoQuant), the delay time of the correlation being limited to the range from 0.15 μs to 0.1 s.

We used rhodamine 6G to calibrate w as a fitting reference. The w was given by a relation of ($D=w^2/4\tau_D$). The parameter of D and τ_D of rhodamine 6G, (w/z), and w were 3.99×10^{-10} m^2s^{-1}, 65.2±3.2 s, 10±0.52, and 322.6±9.8 nm, respectively [17]. The focal volume calculated by the parameters w and (z/w) was 1.8 fL and it was used to calculate sample concentration.

The quantum dots used as the sample had a rod-like shape; therefore, they are called quantum rods. They are classified as Q-rod1, Q-rod2 and Q-rod3 by length. Their width is 6.5± 0.5 nm, and the lengths are 17±3, 40±3 and 46±3 nm for Q-rod1, Q-rod2 and Q-rod3, respectively. The size of each rod was confirmed by TEM, as shown in Fig. 2a, b and c. The method for growing the quantum rods is the same as described in Refs. [18, 19]. The CdSe quantum dot of diameter 3.3 nm becomes to CdSe/CdS nanorods with three different lengths by CdS coating. The same size quantum dot was included inside all of the quantum rods as seed, and all absorbs light with a wavelength shorter than 600 nm and emit fluorescent light of 550 to 650 nm for 532 nm excitation source, as shown Fig. 3.

Before the experiment, we diluted the sample solutions of about 5 μM with distilled water to obtain $G(0)$ of 1 for each sample. By calculation using the focal volume, the concentration of sample quantum rod was found to be about 1 nM.

Results and Discussion

For each case, we obtained fluorescence correlation functions by transferring and averaging the fluorescence intensity fluctuation detected 100 times for 10 s (Fig. 4). Figure 2a and b show cases in which the polarization states of the source and fluorescent light are the same (XXX) and perpendicular (XYY), respectively. The notation of polarization state follows Ref. 7. The results for each rod are represented as Q-rod1, Q-rod2, and Q-rod3. The left and right regions divided by the vertical dotted line are the rotational diffusion region (R) and the translational diffusion region (T). In the translational diffusion region, the decay curve shifts slightly to the right with increasing particle size in both polarization states (Fig. 4a and b). Thus, the translational diffusion time increases with increasing particle size. The quantitative information for

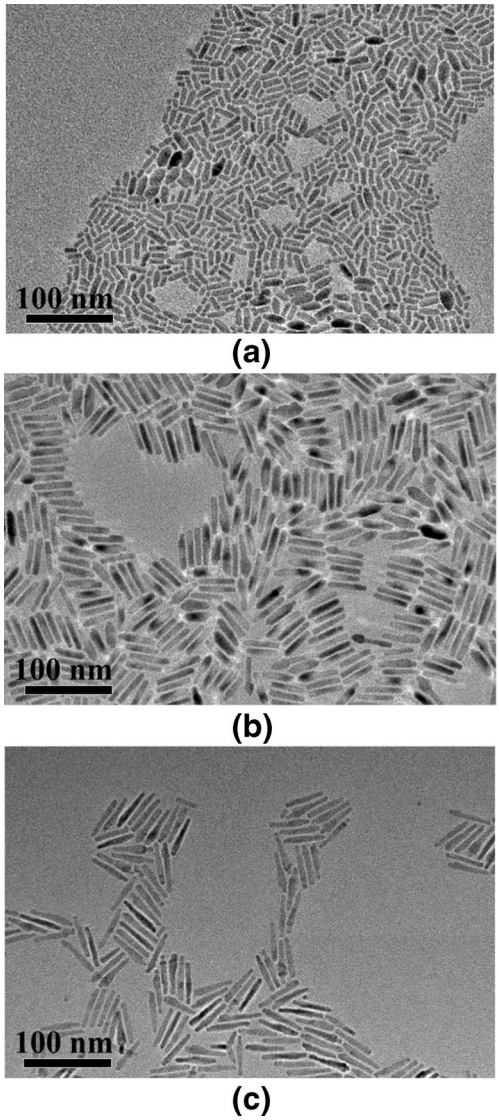

Fig. 2 TEM images of quantum rods. **a** Q-rod1, **b** Q-rod2, **c** Q-rod3

these results can be known by fitting the measured data into Eq. (2) [20]. The parameters, including rotational and translational diffusion time and rotational fraction, were confirmed by fitting. The obtained rotational diffusion times (τ_R) were

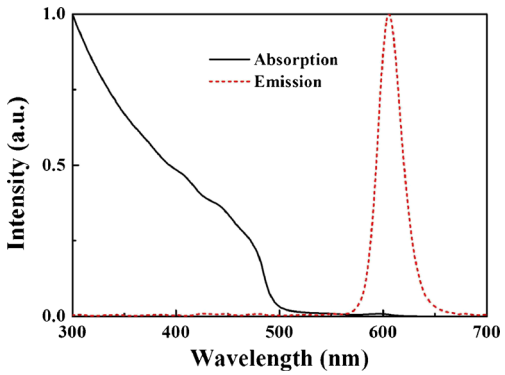

Fig. 3 Absorption and emission spectrum of Q-rod

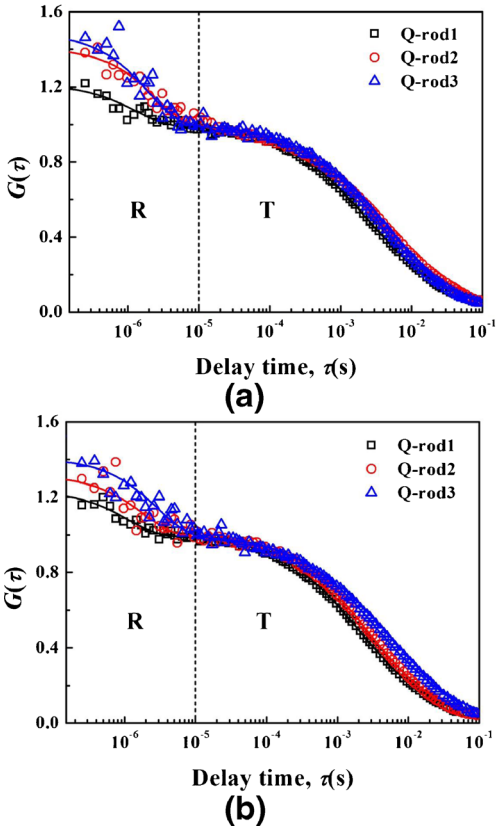

Fig. 4 Fluorescence correlation functions of the three samples. **a** XXX polarization state and **b** XYY polarization state

1.2±0.2, 2.4±0.3, and 2.8±0.3 μs, and the translational diffusion times (τ_D) were 2.4±0.2, 3.4±0.2, and 3.7±0.3 ms for Q-rod1, Q-rod2, and Q-rod3, respectively. The ratio of the lengths of the Q-rods is 1:2.3:2.7; however, the ratio of the rotational diffusion times is 1:2:2.3, and that of the translational diffusion times is 1:1.4:1.5, less than the ratio of the lengths. The reason for these differences in ratios can be determined by analyzing the hydrodynamic radii of the particles. To obtain the hydrodynamic radius, each diffusion time was converted into rotational and translational diffusion coefficients using Refs. 1 and 5.

Figure 5 shows the diffusion coefficients of the rotational region (D_R) and the translational region (D_T) with the length of the Q-rods. Because the diffusion coefficient is proportional to the reciprocal size of the particles, it shows that the values decrease in the order of Q-rod1, Q-rod2, and Q-rod3. The rotational and translational diffusion coefficients are well-known Stokes-Einstein relations as $D_R = k_B T/(8\pi\eta R^3)$ and $D_T = k_B T/(6\pi\eta R)$ [1, 5, 21]. Here, k_B is the Boltzmann constant, T is absolute temperature, η is the viscosity of the solvent, and R is the hydrodynamic radius when the rod is regarded as a sphere. The hydrodynamic radius obtained by substituting the measurement conditions for a temperature of 20 °C and a viscosity of 1.00 cP into the Stokes-Einstein relation was compared with the actual rod size.

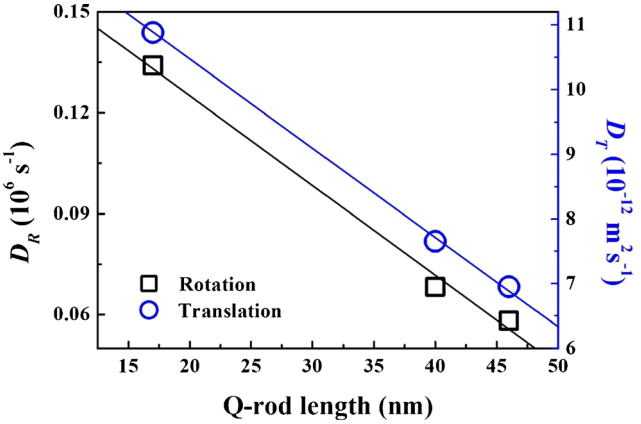

Fig. 5 Rotational and translational diffusion coefficients of Q-rod1, Q-rod2, and Q-rod3

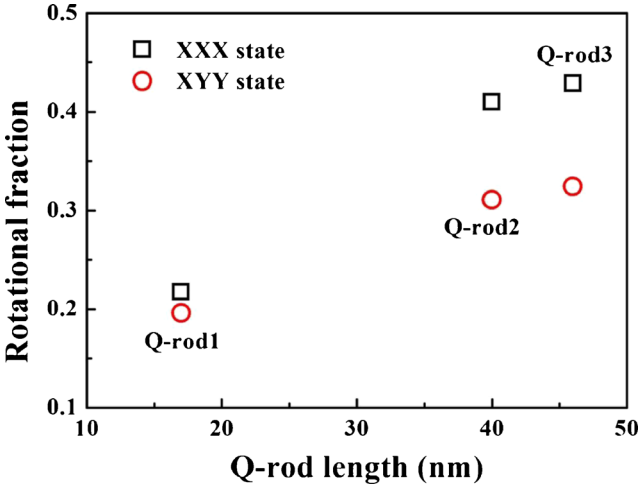

Fig. 6 Rotational fraction for different two polarization states

The radii of the rods were 20.0±3.6, 28.5±1.4, and 31.4±3.1 nm through the translational diffusion coefficient. When the radii of spheres with same volume as the rod samples were calculated using the particle size information provided above, the radii for Q-rod1, Q-rod2, and Q-rod3 were 8.1±0.9, 10.8±1.1, and 11.3±0.9 nm, respectively. This calculated radius was defined as an equivalent radius and used in comparison with the hydrodynamic radius of non-sphere particles [22]. The hydrodynamic radii obtained by the translational diffusion coefficient were three times larger than the equivalent radii because of the effect of blinking in the quantum dot that exists in each quantum rod [23]. The blinking of the quantum dots was considered in various particles in the decay curve of translational diffusion in the correlation function because it is irregular when the particles pass the observation region (focal point). Here, the average translational diffusion time, including blinking, represents the effect of diffusion with larger particles than the actual particles used in our experiments for same reason that the actual length ratio is different from the translational diffusion time ratio presented above. Thus, the hydrodynamic radius cannot be decided by translational diffusion of fluorescent particles based on quantum dots, and only relative information can be obtained when irregular blinking exists.

The hydrodynamic radii calculated using the rotational diffusion coefficients were 10.7±0.8, 13.4±0.7, and 14.1±0.4 nm. All were 3 nm larger than the above-mentioned equivalent radii. If the motion of nano-sized particles slows by friction with the ambient solution, the hydrodynamic radius becomes larger than the equivalent radius [24]. The measured values are about 3 nm larger than the actual size because rod-like particles rotate less stably than spherical particles.

Figure 6 shows the rotational fraction obtained by fitting the signal in each polarization state (XXX and XYY). In each Q-rod, the rotational fraction for the XXX state is larger than for the XYY state. Those results are consistent with the one known by an analysis of the polarized correlation function [7, 25], and they mean that the polarization emission property of a particle appears in the rotational diffusion region. In general, the polarization state of fluorescent light in the translational region is random, and the total average intensity is uniform when the particle passes the observation region. Therefore, the translational fraction was constant. On the other hand, as the rotational fraction shows the variation process of the polarization state by particle rotation in a short time scale, the rotational fraction of the correlation function varies when the polarization states of the source and fluorescence are parallel and vertical. When a rotating polarizer lies between two linear polarizers, this state is divided into two cases. The first and second cases are when the angles between two linear polarizers are zero and 90°, respectively. Both cases show the same rotational relaxation time; however, the intensity fluctuation of the first case is larger than that of the second case [26]. Therefore, as shown in Fig. 6, the larger rotational fraction of XXX state than XYY state is related to the rotating polarizer property of rod-like particles [25]. In the rotational region (Fig. 6), the values of the rotational fraction (R_{XXX}) of Q-rod1, Q-rod2 and Q-rod3 are 0.22, 0.41, and 0.43, and those of R_{XYY} are 0.20, 0.31, and 0.32, respectively. The R_{XXX} is 1.10, 1.32, 1.34 times larger than R_{XYY} and can be related to the ratio of length to width (aspect ratio) of the particles. As mentioned, each particle has a rotational polarizer property, and the rotational fraction is decided by the efficiency of the particles' linear polarizer. If the states of XXX and XYY correspond to the length direction and width direction of the particles, the ratio of the rotational fractions (R_{XXX}/R_{XYY}) in the polarization condition becomes the efficiency of polarization for the length direction of the particles. Figure 7 represents the fraction ratio for two polarization states with particle length and aspect ratio. While the aspect ratio increases linearly, the fraction ratio also increases linearly. Thus, the fraction increases with increasing particle length; however, the detailed properties need to be confirmed by additional study.

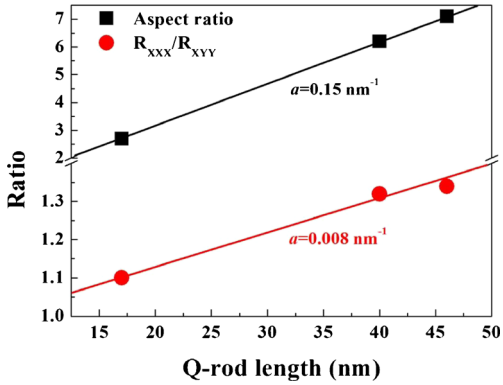

Fig. 7 Variation of ratios by aspect and fraction for polarization states with Q-rod length

This study is usable to analyze a structure change of molecules and protein changed by environmental condition in biomedical field, and to separate different samples of same volume and different aspect ratio such as RNA or DNA folding.

Conclusions

To analyze the variation of correlation function for rotational diffusion with the length of fluorescent particles, we built the polarized FCS-setup. The 3 sample solutions contained quantum rods with a width of 6.4±0.5 nm and lengths of 17±3, 40 ±3 and 46±3 nm. Through the translational and rotational diffusion coefficients of the fluorescent particles, we calculated their hydrodynamic radii. Although the irregular blinking of the quantum dots disturbed the calculation of the hydrodynamic radii in the translational diffusion region, the rotational diffusion region provided hydrodynamic radii of 10.7±0.8, 13.4±0.7, and 14.1±0.4 nm, about 3 nm larger than the equivalent radii. Through fraction analysis by polarization state, we confirmed that the ratio of rotational fraction for polarization increases with the aspect ratio of the actual particle. These results will allow the rotating polarizer properties of quantum rods to be applied usefully in polarization FCS systems.

Acknowledgments This work was supported by the 2015 Research Fund of the University of Ulsan.

References

1. Aragón SR, Pecora R (1976) Fluorescence correlation spectroscopy as a probe of molecular dynamics. J Chem Phys 64:1971
2. Shewille P (2001) Fluorescence correlation spectroscopy and its potential for intracellular applications. Cell Biochem Biophys 34: 383
3. Haustein E, Schwille P (2007) Trends in fluorescence imaging and related techniques to unravel biological information. HFSP J 1:169
4. Haustein E, Schwille P (2003) Ultrasensitive investigation of biological systems by fluorescence correlation spectroscopy. Methods 29:153
5. Araón SR, Pecora R (1975) Fluorescence correlation spectroscopy and Browinan rotational diffusion. Biopolymers 14:119
6. Loman A, Gregor I, Stutz C, Mund M, Enderlein J (2010) Measuring rotational diffusion of macromolecules by fluorescence correlation spectroscopy. Photochem Photobiol Sci 9:627
7. Lee J, Fujii F, Kim SY, Pack C, Kim SW (2014) Analysis of quantum rod diffusion by polarized fluorescence correlation spectroscopy. J Fluoresc 24:1371
8. Dittrich PS, Schwille P (2003) An integrated microfluidic system for reaction, high-sensitivity detection, and sorting of fluorescent cells and particles. Anal Chem 75:5767
9. Han Y, Lee J, Lee Y, Kim SW (2011) Measurement of diffusion coefficients of fluorescence beads and quantum dots by fluorescence correlation spectroscopy. J Korean Phys Soc 59:3177
10. Watanabe TM, Fujii F, Jin T, Umemoto E, Miyasaka M, Fujita H, Yanagida T (2013) Four-demensional spatial nanometry of single particles in living cells using polarized quantum rods. Biophys J 105:555
11. Kask P, Piksarv P, Mets Ü (1985) Fluorescence correlation spectroscopy in the nanosecond time range: Photon antibunching in dye fluorescence. Eur Biophys J 12:163
12. Widengren J, Rigler R, Mets Ü (1994) Triplet-state monitoring by fluorescence correlation spectroscopy. J Fluoresc 4:255
13. Chowdhury PK (2011) Fluorescence correlation spectroscopy: a brief review of techniques and applications to biomolecules and biosystems. J Proteins Proteomics 2:145
14. Lakowicz JR (2006) Principles of fluorescence spectroscopy, Third ed., Springer Science+Business Media. Chapter 24
15. Banks DS, Fradin C (2005) Anomalous diffusion of proteins due to molecular crowding. Biophys J 89:2960
16. Tsay JM, Doose S, Weiss S (2009) Rotational and translational diffusion of peptide-coated CdSe/CdS/ZnS nanorods studied by fluorescence correlation spectroscopy. J Am Chem Soc 128:1639
17. Petrásek Z, Schwille P (2008) Precise measurement of diffusion coefficients using scanning fluorescence correlation spectroscopy. Biophys J 94:1437
18. Carbone L, Nobile C, Giorgi MD, Sala FD, Morello G, Pompa P, Hytch M, Snoeck E, Fiore A, Franchini IR, Nadasan M, Silvestre AF, Chiodo L, Kudera S, Cingolani R, Krahne R, Manna L (2007) Synthesis and micrometer-scale assembly of colloidal CdSe/CdS nanorods prepared by a seeded growth approach. Nano Lett 7:2942
19. Deka S, Quarta A, Lupo MG, Falqui A, Boninelli S, Giannini C, Giorgi MD, Spinella G, Cinglani R, Pellegrino T, Manna L (2009) CdSe/CdS/ZnS double shell nanorods with high photoluminescence efficiency and their exploitations as biolabeling probes. J Am Chem Soc 131:2948
20. Pujol J (2007) The solution of nonlinear inverse problems and the Levenberg-Marquardt method. Geophys (SEG) 72:W1
21. Cooper A (2005) Biophysical Chemistry, RSC. Cambridge. UK. Chapter 4
22. Jennings BR, Parslow K (1998) Particle size measurement: the equivalent spherical diameter royal. Soc Londen Ser A 419:137
23. Peterson JJ, Nesbitt DJ (2009) Modified power law behavior in quantum dot blinking: a Nobel Role for biexcitons and Auger ionization. Nano Lett 9:338
24. Jung C, Lee J, Kang M, Kim SW (2014) Viscosity-dependent diffusion of fluorescent particles using fluorescence correlation spectroscopy. J Fluoresc 24:1785
25. Lee J, Pack C, Kim SY, Kim SW (2014) Diffusion coefficients of CdSe/CdS quantum rods in water measured using polarized fluorescence correlation spectroscopy. J Optom Soc Korean 18: 598
26. Hecht E (2002) Optics, 4th edn. Addison Wesley Longman Inc., United States, Chapter 8